17th World Conference on Earthquake Engineering, 17WCEE
Sendai, Japan - September 13th to 18th 2020

MODELLING OF HISTORIC STONE-DRUM COLUMNS UNDER SEISMIC ACTION

C. Nguyen [(1)], U. Dorka [(2)]

[(1)] *Researcher, Universität Kassel, chuyen.nguyen@uni-kassel.de*
[(2)] *Prof. Dr.-Ing., Universität Kassel, uwe.dorka@uni-kassel.de*

Abstract

The Neptune temple in Italy, a world architectural heritage site, shows some column damage due to seismic events that happened over thousands of years. Although seismic action on such structures is a big concern, there is still not enough scientific knowledge about the behaviour of stone block structures under seismic loading.

The mechanical behaviour of two stone drums in contact is governed mainly by contact mechanics. This can be modelled by defining non-linear hysteresis laws for three orthogonal states: Sliding (in-plane translation), rotating against the vertical axis (torsion) and rotating against the horizontal axis (rocking). To develop this non-linear constitutive law, an FE-model of two half-drums in contact was developed with ABAQUS using 3D elastic solid elements. The local contact was modelled as a thin elastic layer with stick-slip properties. Small-scale friction tests served for specifying the tangential and normal properties of this layer, which are the shear stress limit and contact stiffness. The contact surface obtained with this model, developed during rocking, was compared to the vertical strains measured by strain gauges embedded under the surface of one of the experimental stone drums.

The model was validated by a 1:3 scale test of a multi-drum column from the Neptune Temple. It can now be used with confidence to develop macro elements within the concept of mechanically consistent scaling for the seismic analysis of other Greek column structures that have survived.

Keywords: stone column; seismic; contact modelling; macro element; hybrid simulation;

1. Introduction

There is still a lack of understanding the behaviour of historic structures under earthquakes. But this is a prerequisite for any intervention aiming at improving the seismic performance of these structures. The project reported in this paper deals with the seismic performance of Greek columns as they were built during the classic period. A prime example is the Temple of Neptune in Paestum, Italy (Fig.1). It serves as the lead structure in a joint project between Universität Kassel, Germany and Università degli Studi di Salerno, Italy [1]. Next to understanding and modelling the seismic behaviour of these columns, the project also investigates the effect of the Tendon System as a possible low interference seismic protection system [2].

Fig. 1 – Temple of Neptune in Paestum, Italy, a world heritage site and reference structure for this project.

This article describes a detailed numerical model that represents two column drums in contact under cyclic action. It was developed emphasizing the contact mechanics between the two drums. It has been validated with hybrid simulations [3-5] using a 1:3 scale model of a column from the Temple of Neptune as the specimen. This model was developed within the concept of mechanically consistent scaling [6-9]. That way, complete structures can be modelled with confidence without the need to model each local mechanics in detail.

2. Mechanically consistent scaling

Mechanically consistent scaling [9] requires the identification of a set of orthogonal boundary states for a discrete region. Fig.2 gives some examples. The intrinsic properties of the region are of no concern at this stage.

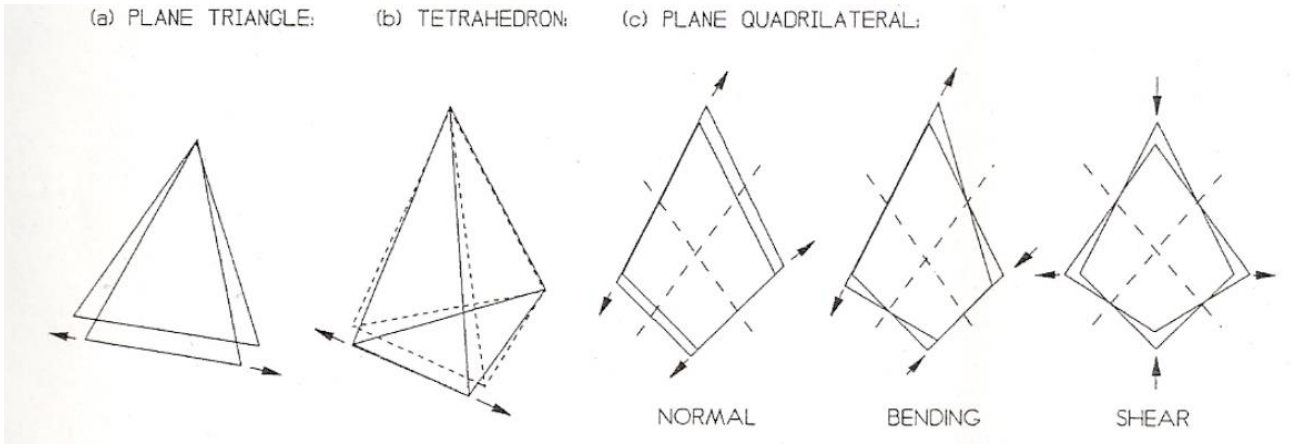

Fig. 2 – Orthogonal boundary states for a plane triangle, tetrahedron and plane quadrilateral with their respective boundary displacements (macro strains) and forces (macro stresses) according to [9]

Orthogonality implies that the macro stresses related to one orthogonal state perform work only on this state, not on the others. The total work done on any state is then the sum of the work done on each orthogonal state, which is represented in their macro stress-strain hysteresis loops. Any state is thus the sum of all existing orthogonal states. A complete constitutive relation for such a region is represented by these macro-stress-strain laws with their parameters coupled through surface laws in the macro-stress space. These constitutive relations depend on the inner mechanics of the region, which may contain voids and exhibit any non-linear behaviour.

The basic equations governing a discrete region are [9]:

$$\varepsilon_k = B_k \cdot u_k \tag{1}$$

$$\sigma_k = D_k \cdot \varepsilon_k \tag{2}$$

$$f_k = B_k^T \cdot \sigma_k \tag{3}$$

$$K_k = B_k^T \cdot D_k \cdot B_k \tag{4}$$

for the k^{th} macro element.

Eq. (3) and (4) can be derived from the stationarity of the potential of a discrete region by utilizing Eq. (1) and (2). The matrix B_k contains the transformations from nodal displacements to macro strains and is a geometric property of the macro element. D_k represents the constitutive relation, which is usually non-linear. Eq. 4 provides the stiffness matrix if D_k is constant (linear mechanics).

The method was applied in the development of a macro element for a frame corner in steel-concrete composite frames under static loading [6-8]. A rectangular quadrilateral was used (compare Fig.2). Its constitutive relation was based on a detailed FE-model of the corner capable of representing (among others) yielding in the web corner, failure of welds as well as cracking in the concrete deck.

When applied to two stone column drums in contact, three orthogonal states can be identified that form a complete set: Rocking, sliding, and torsion (Fig.3). The principal macro-stress-strain hysteresis loops (M_θ-θ for rocking, V-δ for sliding and M_ϕ-ϕ for torsion) may exhibit pinching. They can be coupled in the macro-stress space with a two-surface law, where the sizes of the surfaces depend on normal force N (isotropic hardening rule) and their location in the macro-stress space on the loading history (kinematic flow rule).

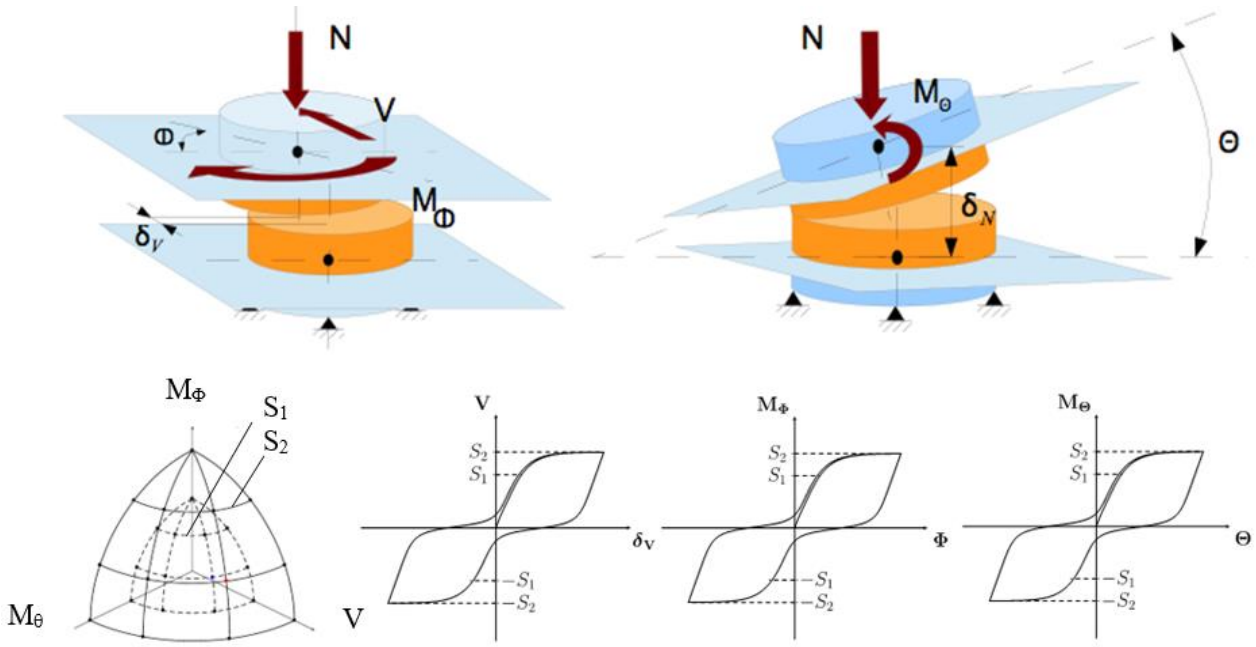

Fig. 3 – Orthogonal states for a macro element representing two drums in contact (top: rocking M_θ-θ, sliding V-δ, torsion M_ϕ-ϕ) and the principal description of the constitutive relation for this macro element (bottom).

The constitutive relation for this macro element can be taken directly from experiments, which can also be used to validate a detailed FE-model that faithfully represents the local contact mechanics in particular.

3. A detailed numerical model for two drums in contact

According to the principals of mechanically consistent scaling, the macro element boundaries are selected at the centre planes of the drums. Non-linear behaviour within the drums is not expected and therefore neglected. It is concentrated in the interface between the drums, which therefore needs special attention. ABAQUS v.12-3 [10] was used to set up this model, allowing for very sophisticated modelling of the interface, if required.

This model is general in the sense that its overall dimensions and material properties can be selected as needed. In this study, they were taken from the specimen to enable validation. It was made of travertine stone with elastic modulus E = 55 GPa [11], Poisson ratio ν = 0.2 and density ρ = 2440 kg/m^3.

Fig.4 provides details on the model. The two half-drums are modelled as two deformable solids using 3D elastic brick elements of type C3D8R (8 nodes, three-dimensional brick, linear reduced integrated element [12]) for the main body of the drums. Reference points (RPs) are set at the centres of the boundary planes to control their motion and keep them plane. Loading (N) and boundary displacements can now be applied through the RPs. A finer mesh was created near the contact surface to allow for the analysis of stress concentrations, especially at the edge. Here, elements of type C3D20R (20 nodes, three-dimensional brick, linear reduced integrated element [12]) were used, providing a better resolution than the C3D8R. In total, the model has 6400 C3D8R elements and 2560 C3D20R elements.

The contact between the two half-drums is modelled using the "contact pair approach" in ABAQUS [12]. In this approach, a "pair" has two surfaces in contact, each inheriting the deformations of the adjacent elements. In ABAQUS non-penetration constraints are applied at specific nodes on these interacting surfaces. The locations of these nodes depend on the nodes of the elements adjacent to a "pair". One surface of a "pair" is set as master and the other as slave. Master nodes cannot penetrate the slave surface. These model surface contact in an average sense. In the model for the two drums, the 8-node C3D8R elements in the upper drum define the master nodes.

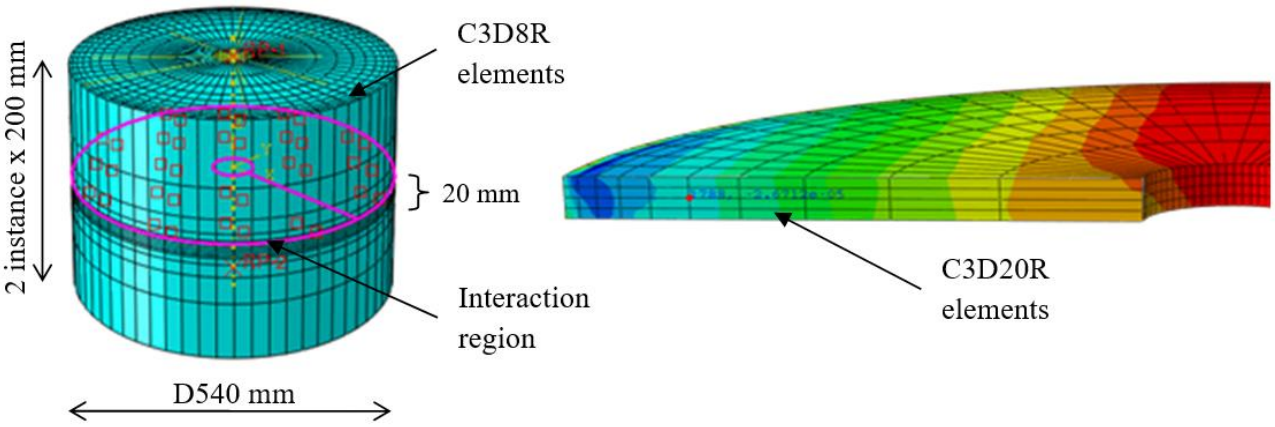

Fig. 4 – Detailed local FE-model set up with ABAQUS. Measures are taken from column specimen to enable validation. There are 4 layers of high-resolution elements (right) on both sides of the contact surface to allow for a detailed analysis of stress concentrations there.

Contact modelling poses particular challenges: The local surface is not plane, has voids and material properties vary considerably. To provide more general model again, it is necessary to use some simplifying assumptions. These are: -the contact surface is plane, -simple isotropic Coulomb friction applies, -vertical in-plane deformations occur near the surface but remain elastic. Under these conditions, simple horizontal and vertical constitutive relationships can be used to model the contact mechanics within a "pair". Fig.5 shows the piece-wise linear hysteretic shear-slip and quasi-elastic pressure-overclosure relationships that were assumed for a "pair".

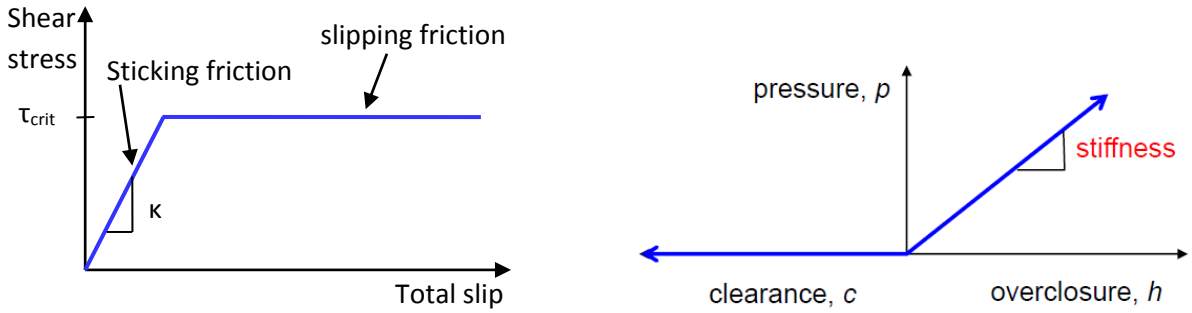

Fig. 5 – Relationships for tangential (left) and normal behaviour (right) to model the contact mechanics of a "pair"[12]

The pressure – overclosure stiffness (Fig.5 right) is set by default to 10 times an adjacent representative element stiffness. This is not only a reasonable assumption to model the mutual penetration of surfaces in contact due to their asperities, but also to provide numerical stability.

To determine the parameters of the shear - slip relationship (Fig.5 left), small-scale friction tests were conducted.

4. Small-scale friction tests

4.1 Specimens and test setup

Three travertine cylinders were extracted from the drums of the column specimen and used as specimens for these tests (Fig.6). The middle core has the following dimensions: length L = 90 mm, diameter D = 64.5 mm, section area 3265 mm^2. The two side cores have length L = 30 mm and diameter D = 64.5 mm. They are held by steel rings that allow them to move only horizontally. The surfaces of all cylinders were grinded flat.

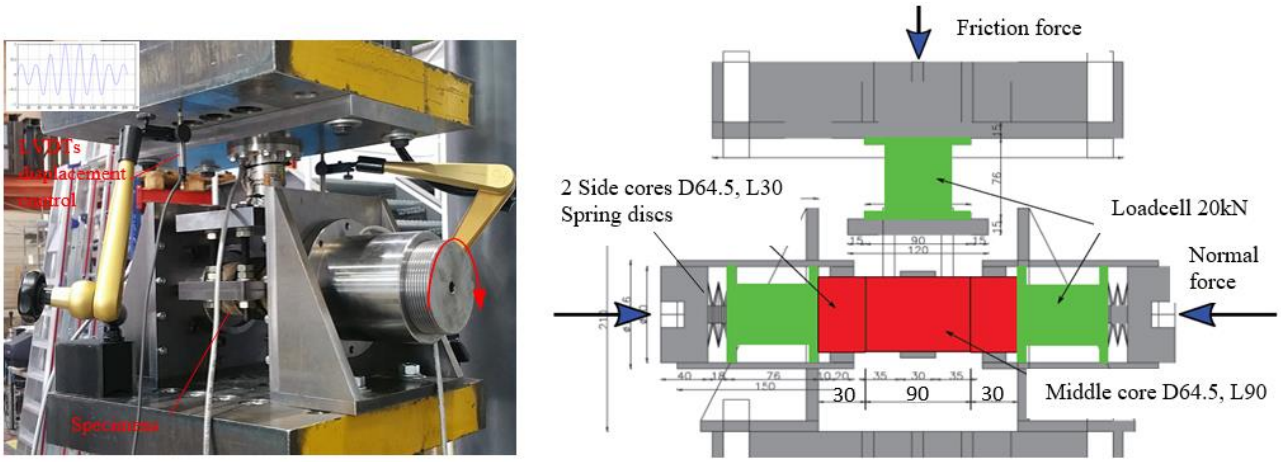

Fig. 6 – Small-scale friction test setup with travertine cylinders (red side - and middle cores)

Normal and friction forces were measured with three load cells of 20 kN each (green, Fig.6 right). Normal forces were applied by turning the large screws at the ends of the horizontal steel tubes (Fig.6 left). These forces were controlled using disc springs (62x18x2.0 mm, H = 4.85 mm) within the tubes. These springs have a non-linear elastic characteristic, which keeps the spring force nearly constant over a certain deformation range [13].

4.2 Testing program

The tests were displacement controlled. Two high-resolution displacement gauges type WI/5mm-T [15] were installed to control the sliding motion between the middle and side cores. A sine loading function was used based on the cyclic testing procedure presented in [14], which allows the analysis of a specimen's performance also during cyclic unloading (Fig.7). This function can be applied repeatedly with increasing or varying centre amplitudes. This allows the creation of different loading histories as required.

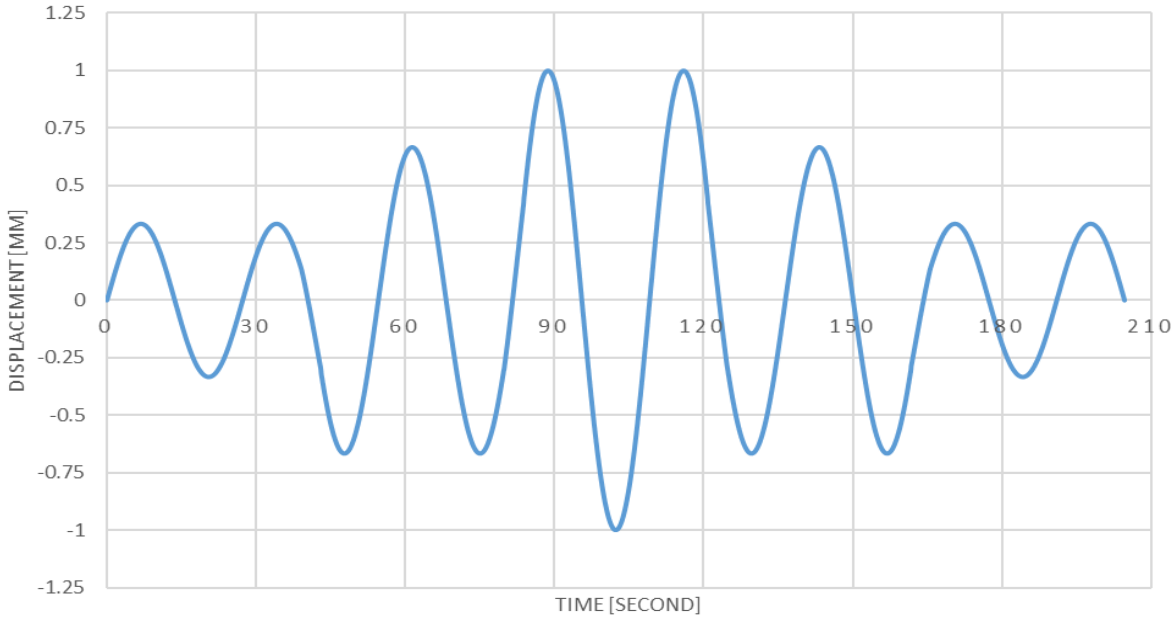

Fig. 7 – Sine loading function for all friction tests based on [14].

Four friction tests were conducted, each with three normal force levels: 1.0 kN, 1.6 kN and 2.0 kN. These normal forces resulted in compressive stresses of 0.3 MPa, 0.5 MPa and 0.6 MPa respectively. They correspond to stress levels reported in the column tests [2].

4.3 Results

Fig.8 shows the specimen after testing. Only minimal wear was observed under these realistic surface pressure conditions validating the basic assumptions made for the numerical model (Fig.4).

Fig. 8 – Minimal wear on the contact surfaces after the friction tests

Fig.9 shows a hysteresis loop representative of these tests. They allowed the determination of the parameters for the simplified shear-slip relationship given in Fig.5.

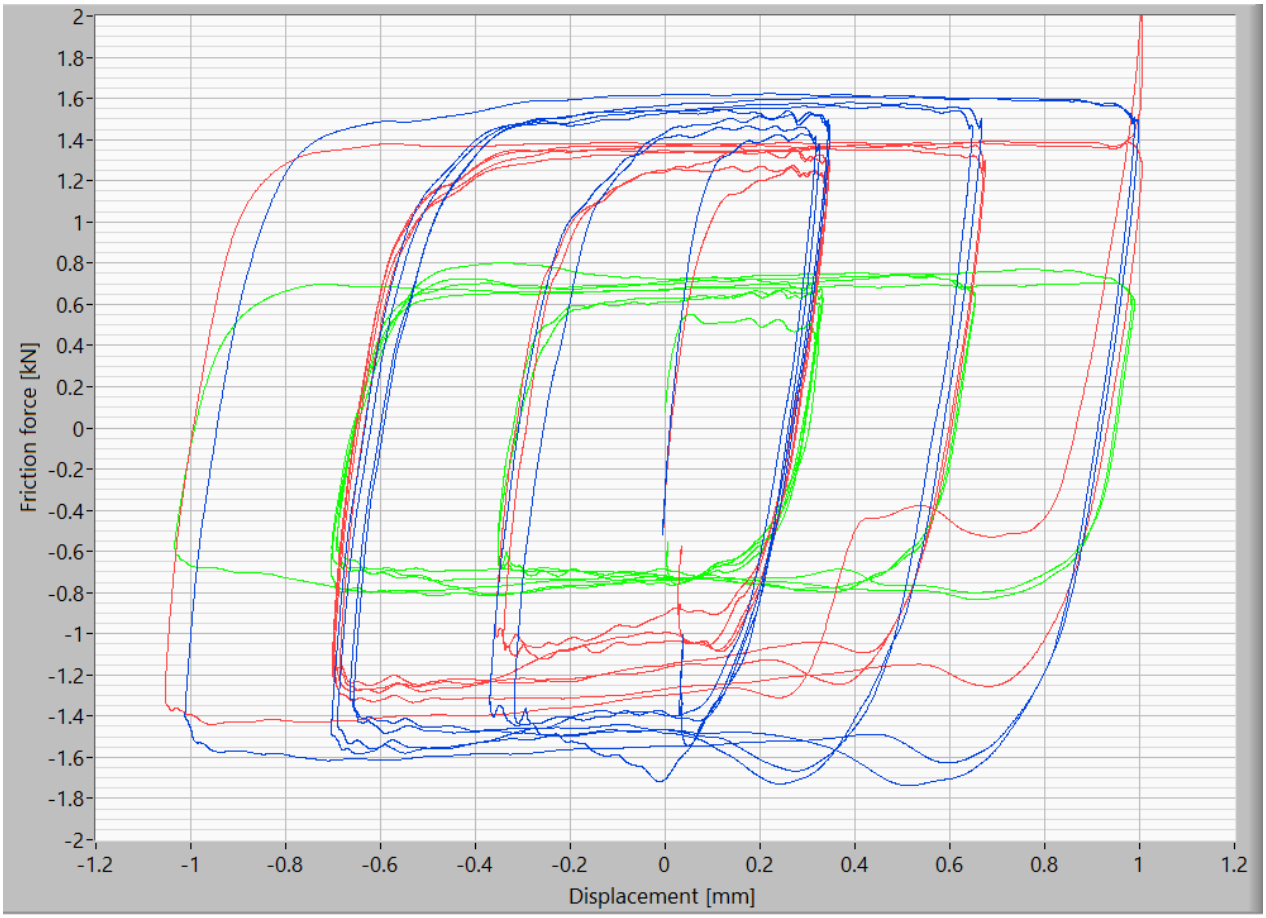

Fig. 9 – Hysteresis loop with three levels of normal force: 1.0 kN (green), 1.6 kN (red) and 2.0 kN (blue)

The coefficient of friction μ has been determined in the range between 0.72 - 0.87. In the numerical model, μ is chosen as the average of 0.75. The shear - slip stiffness κ has been determined from these loops to be 14300 N/mm.

5. Validation of the detailed numerical model with column tests

5.1 Temple of Neptune hybrid simulations

The specimen in the laboratory at the University of Kassel was a 1:3 replica of a column of the Temple of Neptune in Paestum, Italy (Fig.1). The column consists of a base stone followed by six drums, which are topped by abaqus, echinus and an architrave (Fig.10 left). The architrave serves as a load introduction system, with five hydraulic cylinders connected to it. Four of the cylinders (no. 1 - 4) are in displacement control while vertical cylinder no. 5 controls the total vertical force. Hybrid simulations using the Subfeed approach [4, 5] were performed under earthquake loading: A highly complex, non-linear numerical model of the temple was connected online to the specimen. For further details on these simulations, the reader is referred to [2].

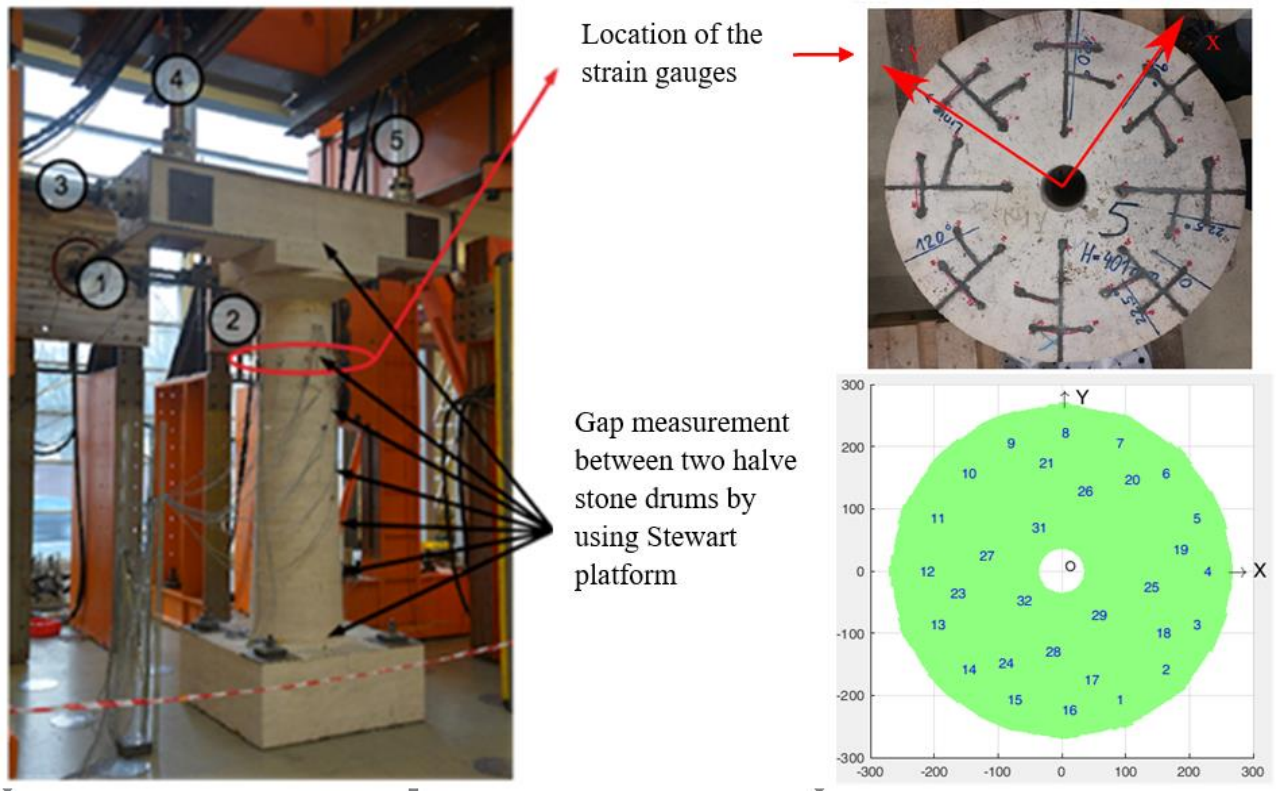

Fig. 10 – (left) Column test setup; (right) Circular array of 32 embedded strain gauges

On the lower surface of the fifth stone drum, a set of 32 strain gauges HBM 1-LY11-3/350 [17] was embedded in a circular array (Fig.10 right). The strain gauges were applied to the wall of holes with a diameter of 10 mm and a depth of 20 mm. They were placed at a depth of 10 mm to measure vertical strains. The holes were filled with Ultra-High Performance Concrete with an elastic modulus of 53 GPa, which is similar to the travertine. Detailed investigations on this strain gauge arrangement showed that this ensures the minimization of strain concentrations around such holes and provides vertical strain measurements within such a solid with excellent accuracy [18].

The relative motion between two drums was measured by a group of six high precision LVDTs with a resolution of 5 µm, arranged as Steward Platform [16]. This platform was installed between the central planes of two drums to measure three displacements (U_x, U_y, U_z) and three rotations (R_x, R_y, R_z). The platform could be moved to other pairs of consecutive stone drums.

5.2 Comparison between the numerical model and test results

The Stewart platform measurements were used as input displacements to the numerical model so that the global (boundary forces and moments: global hysteresis) and local (near-surface strains) response of two drums in contact could be compared. The results shown here are from a hybrid simulation using the Petrovac 1979 earthquake scaled to 1.2g (test_7 in [2-4]). The normal force was kept constant during this simulation. It was 81 kN on the fifth stone drum.

Fig.11 shows the comparison between a single strain measurement (strain gauge 7) and its associated strain from the numerical model (node 1788). Both show essentially the same behaviour over time, with some divergence towards the end of the test, which needs further studying.

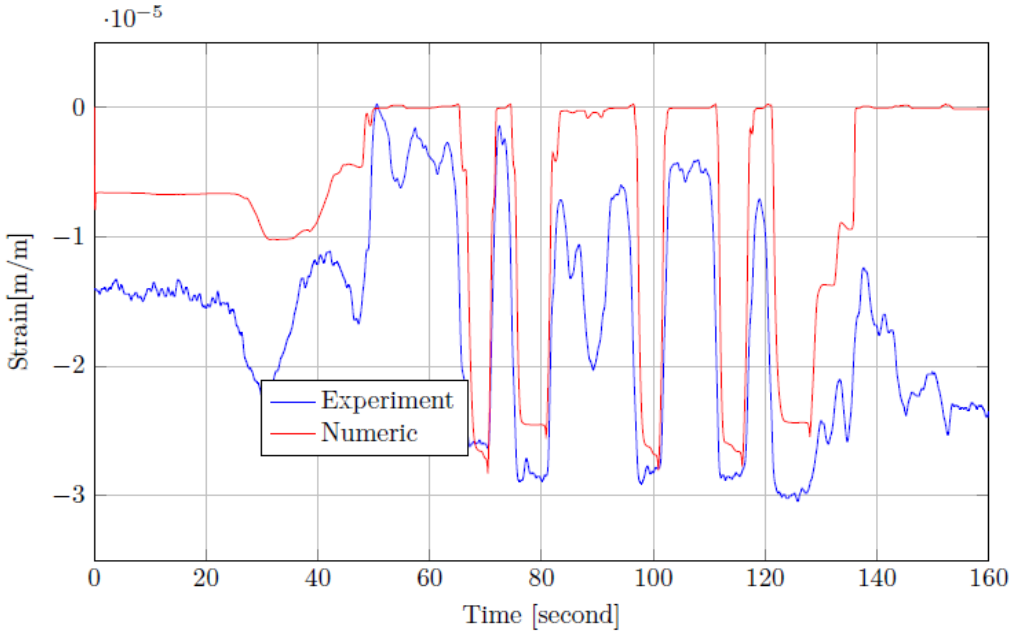

Fig. 11 – Measured vertical strain at strain gauge number 7 and numerical model vertical strain at node 1788 – Hybrid Simulation test_7

Peak values are almost the same and occur at the same time. At these points in time, sub-surface strain distributions can be compared between measurements and numerical model (Fig.12).

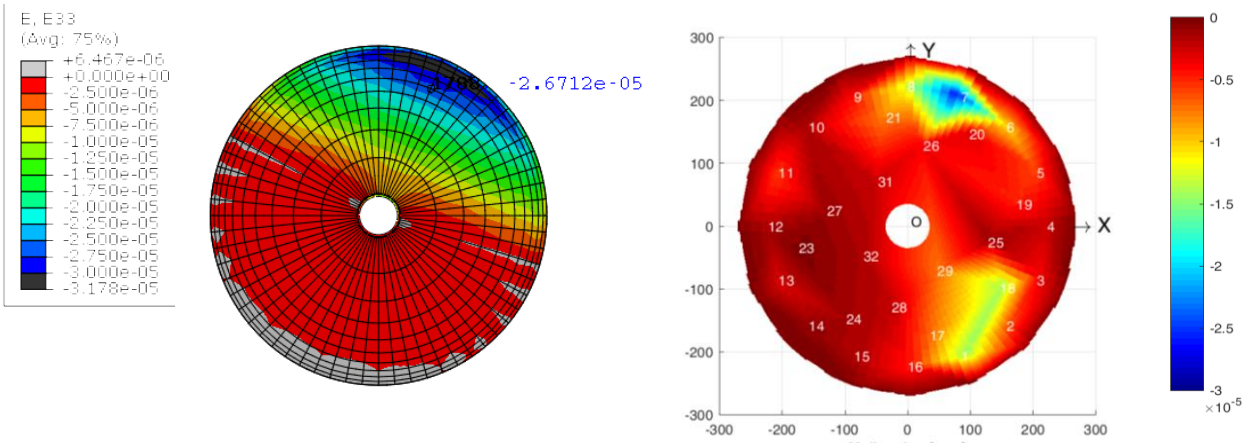

Fig. 12 – Comparison of sub-surface vertical strain distributions at the t = 69.5s peak, unit m/m: Experiment (top); numerical simulation (bottom).

Although it captures the position and value of the peak strain quite well, the numerical model tends to spread the strains over a wider area. This can be explained by the un-evenness of the real surfaces, which results in a more concentrated and less even distribution: Note the secondary concentration in the measurements almost opposite to the main peak (green area at lower right).

The measurements from the Stewart Platform showed that rocking is the dominant motion, with the orthogonal states of sliding and torsion being essentially negligible. Therefore, the following comparison for the global hysteresis concentrates only on this orthogonal state (see Fig.3, top right). Noting that the direction of rocking changes over time, the two bending moments (M_x and M_y) and rotations (R_x and R_y) must be combined to arrive at the orthogonal rocking state M_θ-θ. Fig.13 gives the comparison of the numerical results with the measurements showing an excellent match.

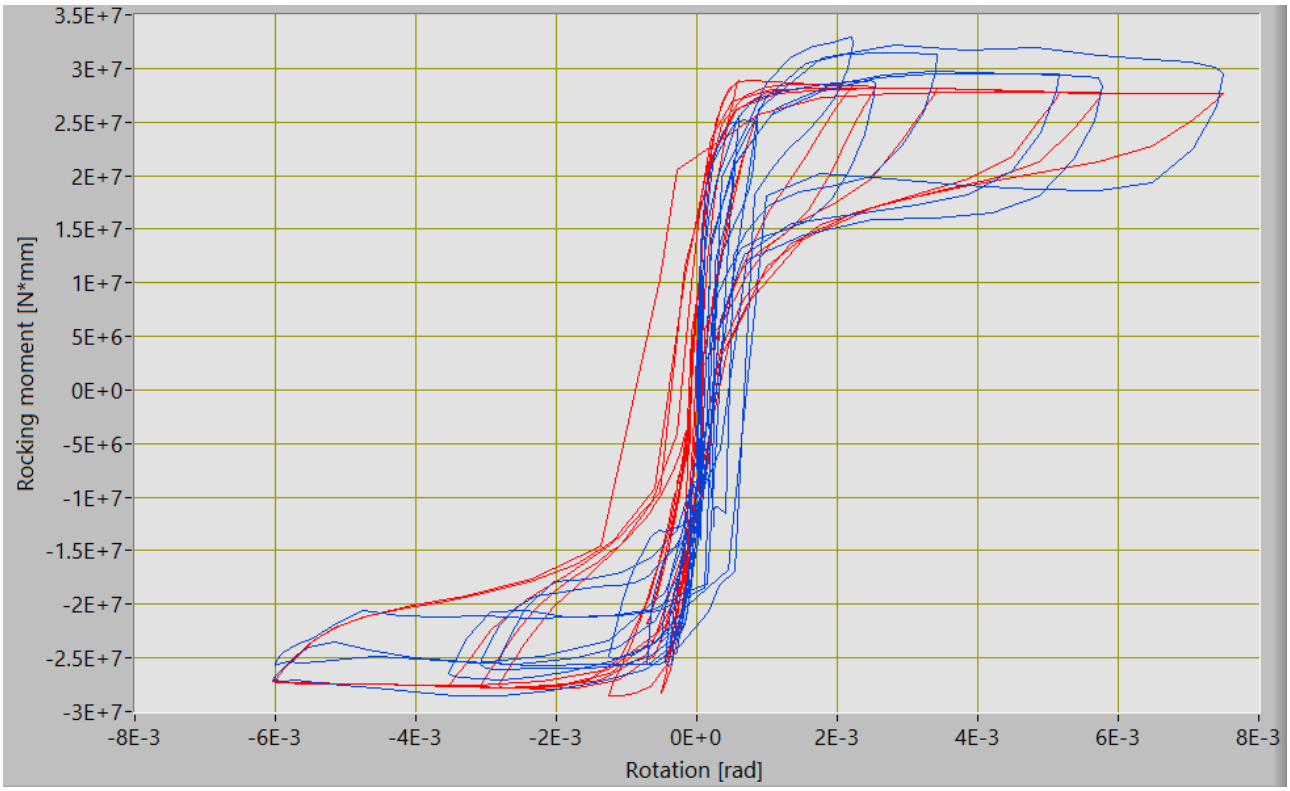

Fig. 13 – Comparison of the numerical model (red) and experiment (blue) for the orthogonal rocking state: Rocking moment M_θ- Rotation θ

6. Conclusions and Outlook

A detailed numerical model has been developed for two stone drums in contact that matches experimental results with sufficient accuracy considering that the properties of real-life stone drum surfaces may vary widely (evenness, voids, local defects etc.). It may now be used with confidence to model similar drum configurations under cyclic action, provided that the relevant surface contact properties are known, which are the shear – slip and pressure – overclosure relationships. Using Finite elastic elements for the main body of the drums is warranted since stresses under regular loading (dead load, wind, etc.) are well below any stress limits of typical materials for such drums.

Even under the dominant rocking motion that will occur under severe earthquake loading, local stress concentrations remain in the elastic range although edges may suffer some negligible damage. Wear in the

contact surfaces is minimal. This validates the developed model even for studies dealing with severe seismic actions.

The model can now be used to develop macro models for two drums in contact within the concept of mechanically consistent scaling. This is done by providing rheological models for the hysteresis loops of the three orthogonal states (dominant rocking, sliding and torsion) and a surface law that connects them. When using such macro elements in system analysis, it is not only numerically very efficient, but local behaviour (like local strains) can be retrieved at any time by applying the orthogonal states to the detailed model developed here.

7. Acknowledgements

The authors of this paper would like to thank the German Research Foundation (DFG) for the financial support of this project: Tendon Systems for Seismic Protection of Stone Block Historical Structures DO-360/25-1.

8. References

[1] DFG Project (2014-2016): Tendon Systems for Seismic Protection of Stone Block Historical Structures DO-360/25-1 (TeSSPACS).

[2] F. Obón Santacana, U. E. Dorka, C. Nguyen and L. Petti (2017): Behaviour of Greek Columns during Earthquakes with and without Tendon System. *3rd International Conference on Protection of Historical Constructions*. Lisbon, Portugal.

[3] F. Obón Santacana, U. E. Dorka, L. Petti (2017): Hybrid Simulation in Combination with Highly Complex and Non-Linear Numerical Models for Seismic Protection of Antique Column Structures. *16th World Conference on Earthquake Engineering.* Santiago Chile.

[4] U. E. Dorka, F. Obón Santacana (2017): Hybrid Simulation using the Subfeed in Highly Complex and Non-Linear Numerical Models. *7th International Conference on Advances in Experimental Structural Engineering.* Pavia, Italy.

[5] Roik K., Dorka U. E. (1989): Fast online earthquake simulation of friction-damped systems. Berichte / SFB 151. Sonderforschungsbereich Tragwerksdynamic Ruhr-Universität Bochum, Germany.

[6] U. E. Dorka, Saenboon Amorntipsakul (2008): Macro-Elements for Composite Beam-Column Connections. *The Conference Composite Construction in Steel and Concrete VI.* Colorado, USA.

[7] S. Amorntipsakul, U. E. Dorka (2008): Generic Finite Element local model for the composite beam-column joint with the welded connection. *Composite Construction VI.* Devil's Thumb, Colorado, USA.

[8] Uwe E. Dorka (2009): Scaled Analysis of Steel-Concrete Composite Beam-Column Connections. *9th International Conference on Steel-Concrete Composite and Hybrid Structures.* Leeds, UK.

[9] U. E. Dorka (1991): System analysis by discrete elements. *The Asian Pacific Conference on Computational Mechanics.* Hong Kong, 1257-1262.

[10] https://www.3ds.com/products-services/simulia/products/abaqus/abaquscae/

[11] A. Reim (2015): Travertine compression test. *Technical Report*. AMPA, University of Kassel.

[12] Abaqus v6.12 (2012): Abaqus analysis user's guide. Dassault Systèmes.

[13] Uwe E. Dorka (1988): Ein Beitrag zur Beurteilung und vereinfachten Berechnung von Bauwerken unter Berücksichtigung der Hysterese-evolution. *Technical Report.*

[14] U. E. Dorka, J. Garcia, R. T. Severn, R. Bairrão (2005): Seismic qualification of passive mitigation devices. *Report no. 1*. ISBN 972491965X, 9789724919652

[15] https://www.hbm.com/fileadmin/mediapool/hbmdoc/technical/B01119.pdf

[16] Charles C. Nguyen, Sami C. Antrazi, Zhen-Lei Zhou and Charles E. Campbell (1991): Analysis and implementation of a 6 DOF Stewart platform-based robotic wrist. *Computers Elect. Engng*, **17** (3), 191-203.

[17] https://www.hbm.com/de/4561/ly-lineare-dehnungsmessstreifen-mit-1-messgitter/

[18] Christophe Poeckes (2016): Beitrag im Rahmen des DFG "TESSPACS-Projekts" zur Quantifizierung der Einflussgrößen von Störzonen aufgrund integrierter Dehnungsmessstreifen (DMS) an einer Versuchssäule. *Master's Thesis*. The University of Kassel.

